

Field-Based Stable Isotope Analysis of Carbon Dioxide by Mid-Infrared Laser Spectroscopy for Carbon Capture and Storage Monitoring

Robert van Geldern,^{*,†} Martin E. Nowak,^{‡,§} Martin Zimmer,[‡] Alexandra Szizybalski,[‡] Anssi Myrntinen,[†] Johannes A. C. Barth,[†] and Hans-Jürg Jost^{||}

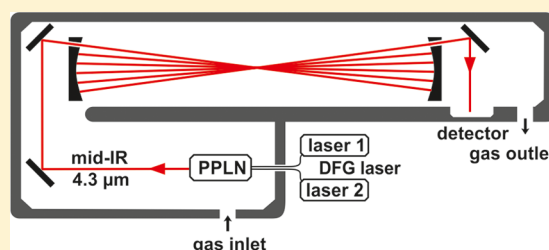
[†]Department of Geography and Geosciences, Friedrich-Alexander University Erlangen-Nürnberg, GeoZentrum Nordbayern, Schlossgarten 5, 91054 Erlangen, Germany

[‡]GFZ German Research Centre for Geosciences, Telegrafenberg, 14473 Potsdam, Germany

[§]Max-Planck Institute for Biogeochemistry, Hans-Knöll Strasse 10, 07745 Jena, Germany

^{||}Thermo Fisher Scientific, Hanna-Kunath-Strasse 11, 28199 Bremen, Germany

ABSTRACT: A newly developed isotope ratio laser spectrometer for CO₂ analyses has been tested during a tracer experiment at the Ketzin pilot site (northern Germany) for CO₂ storage. For the experiment, 500 tons of CO₂ from a natural CO₂ reservoir was injected in supercritical state into the reservoir. The carbon stable isotope value ($\delta^{13}\text{C}$) of injected CO₂ was significantly different from background values. In order to observe the breakthrough of the isotope tracer continuously, the new instruments were connected to a stainless steel riser tube that was installed in an observation well. The laser instrument is based on tunable laser direct absorption in the mid-infrared. The instrument recorded a continuous 10 day carbon stable isotope data set with 30 min resolution directly on-site in a field-based laboratory container during a tracer experiment. To test the instruments performance and accuracy the monitoring campaign was accompanied by daily CO₂ sampling for laboratory analyses with isotope ratio mass spectrometry (IRMS). The carbon stable isotope ratios measured by conventional IRMS technique and by the new mid-infrared laser spectrometer agree remarkably well within analytical precision. This proves the capability of the new mid-infrared direct absorption technique to measure high precision and accurate real-time stable isotope data directly in the field. The laser spectroscopy data revealed for the first time a prior to this experiment unknown, intensive dynamic with fast changing $\delta^{13}\text{C}$ values. The arrival pattern of the tracer suggest that the observed fluctuations were probably caused by migration along separate and distinct preferential flow paths between injection well and observation well. The short-term variances as observed in this study might have been missed during previous works that applied laboratory-based IRMS analysis. The new technique could contribute to a better tracing of the migration of the underground CO₂ plume and help to ensure the long-term integrity of the reservoir.



Anthropogenic CO₂ emissions to the Earth's atmosphere are estimated for 2013 with (9.9 ± 0.5) PgC year⁻¹ from fossil-fuel combustion and cement production and (1.0 ± 0.5) PgC year⁻¹ from land-use change, namely, deforestation.¹ Overall, cumulative anthropogenic emissions from 1840–2013 sum up to (353 ± 55) PgC and are regarded as a major contributor to global climate change.² Atmospheric CO₂ concentrations exceeded 400 μatm at Mauna Loa Observatory in May 2013.³ Within this context, carbon capture and storage (CCS) technologies represent a considerable tool in a portfolio of different reduction methods to mitigate CO₂ emissions on a global and climate-relevant scale.⁴

Stable isotope analyses provide a powerful tool to trace the fate of CO₂ in the subsurface.^{5–8} Stable isotopes of injected CO₂ can act as useful tracers in CCS because the CO₂ itself is the carrier of the tracer signal and remains unaffected by sorption or partitioning effects. In addition, carbon stable isotopes can be used to unravel the role of subsurface processes such as carbonate

mineral dissolution or dissimilatory bacterial sulfate reduction (BSR) that can influence the isotope geochemistry of the injected CO₂.⁹ Therefore, isotope techniques can help to improve our understanding about processes in the subsurface during CO₂ injection and to increase the applicability of reservoir safety monitoring programs.

Over the last years the introduction of a new class of commercially available laser instruments that use near-infrared spectroscopy have revolutionized stable isotope analyses. This technology is frequently referred to as isotope ratio infrared spectroscopy (IRIS)^{10–12} or laser absorption spectroscopy (LAS).^{13,14} These new instruments tend to increasingly replace traditional isotope ratio mass spectrometry (IRMS) that served for decades as the gold standard in stable isotope analysis. This is

Received: August 23, 2014

Accepted: November 6, 2014

Published: November 6, 2014

particularly true for oxygen and hydrogen stable isotope analysis of water.^{12,14,15} A number of studies started to use laser instruments for field monitoring of stable isotope analyses of carbon dioxide or methane for leak detection at CO₂ underground storage sites^{16,17} or along natural gas pipelines.^{18,19}

Compared to IRMS instruments that require a relatively large space in a temperature-controlled laboratory, the new laser instruments are more robust, smaller in size, and can be installed even in remote sites for direct field measurements. This enables high-resolution, real-time in situ measurements that help to investigate processes that otherwise could not be monitored.

Currently, market relevant commercially available laser instruments use the near-infrared region and rely either on cavity ring-down spectroscopy (CRDS; Picarro Inc., Santa Clara, CA, U.S.A.) or off-axis integrated cavity output spectroscopy (OA-ICOS; Los Gatos Research Inc., Mountain View, CA, U.S.A.). Both require comparatively long optical effective path lengths of up to several kilometers due to the absorption characteristics in this part of the optical spectrum. The performance of these instruments have been described, for example, by Vogel et al.²⁰ or Wen et al.¹¹ In addition, optical instruments are available that use quantum cascade laser absorption spectroscopy (QCLAS; Aerodyne Research Inc., Billerica, MA, U.S.A.), Fourier transform infrared spectroscopy (FT-IR; Ecotech Pty Ltd., Knoxville, Victoria, Australia), or the older, discontinued tunable-diode laser absorption spectrometer TGA200 (TDLAS; Campbell Scientific Inc., Logan, UT, U.S.A.) (see also review by Griffis²¹).

During this study an entirely new isotope ratio mid-infrared spectrometer (Delta Ray, Thermo Fisher Scientific, Bremen, Germany)²² was tested for the first time in a field-based tracer study. Compared to cavity-enhanced instruments that operate in the near-infrared, the mid-infrared offers several advantages. The mid-infrared technique allows for a short effective path length of only ~5 m because the associated line strength is approximately 8000 times stronger than in the near-infrared region. This much stronger absorption feature also results in a generally higher precision in the same averaging time compared to the near-infrared. The short path length and relatively simple direct absorption approach allows for a portable, compact, and robust instrument design. Furthermore, the much simpler multipass setup does not require ultraclean, high-reflective mirrors that are required by the long path lengths of cavity-enhanced instruments.

In order to test performance and accuracy of the new mid-infrared laser analyzer, it was installed at the Ketzin pilot site for CO₂ storage in northern Germany in August 2013. The instruments continuous stable isotope record was accompanied by daily CO₂ sampling for laboratory-based IRMS analysis. Both results are compared in this study to demonstrate the high precision and accuracy of the field deployable mid-infrared laser analyzer under outside laboratory conditions. Furthermore, it was evaluated if the continuous stable isotope monitoring technique would provide new insights into underground geochemical processes and subsurface migration of the CO₂ plume.

EXPERIMENTAL SECTION

Experimental Setup at the Study Site. The Ketzin pilot site is located 40 km west of Berlin, in the northeastern part of Germany. Ketzin is the longest operating injection site in Europe. Details of the pilot site are described in Martens et al.²³ and Martens et al.²⁴ At the facility a total of 67 271 tons CO₂ were

injected between June 2008 and August 2013. The average CO₂ injection rate was about 1350 tons per month.²³ The CO₂ was injected in supercritical state in the Ketzin anticline at depths between 632 and 645 m below ground level (bgl) into a heterogeneous saline aquifer sealed by an overlying more than 150 m thick mudstone-dominated cap rock. Observation wells around the injection well ensure a continuous in situ monitoring of the CO₂ storage reservoir²⁵ (Figure 1).

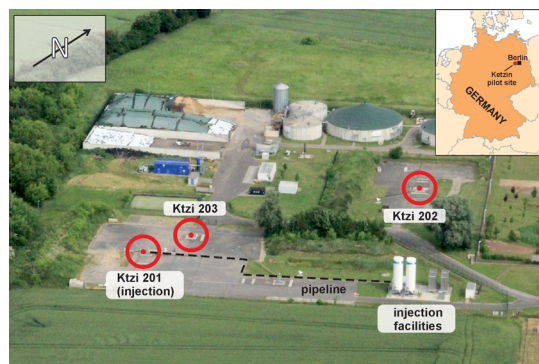


Figure 1. Aerial photograph of the Ketzin pilot site. CO₂ is injected at injection well Ktzi 201. The monitoring instruments of this study were connected to a stainless steel riser tube that was installed in observation well Ktzi 203 at 600 m below ground level (bgl). The distance between Ktzi 201 and Ktzi 203 is ~20 m. Aerial photograph adapted with permission from copyright holder GFZ German Research Centre for Geosciences (Helmholtz Centre Potsdam), Germany. Inset created using WolframAlpha Pro [Wolfram Alpha LLC, 2014, <http://www.wolframalpha.com/input/?i=Germany%20map> (accessed June 3, 2014)].

Previous studies have shown that batches of isotopically distinct CO₂, which has been injected sporadically at the Ketzin pilot site, could be used as a tracer for CO₂ migration in the reservoir.⁵ For this study, 500 tons of CO₂ from a natural CO₂ reservoir ($\delta^{13}\text{C}_{\text{CO}_2} \approx -3.5\text{‰}$ vs VPDB) had been coinjected with N₂ between August 2 and 13, 2013. The $\delta^{13}\text{C}$ value of the natural source CO₂ was significantly different from background values in the reservoir ($\delta^{13}\text{C}_{\text{CO}_2} \approx -28.5\text{‰}$) and has been expected to generate an identifiable isotope tracer breakthrough signal at an observation well several days after injection. In order to observe the breakthrough of the isotope tracer continuously, the instruments were connected to a stainless steel riser tube that was installed in an observation well (Ktzi 203) at 600 m bgl. Formation pressure continuously lifts CO₂ from the storage formation to the surface. Details of the riser tube are described in Nowak et al.⁵ This observation well (Ktzi 203) has a distance of ~20 m to the injection well (Ktzi 201). The riser tube was connected to a GC-TCD/HID analysis system (SRI Instruments Inc., Torrance, CA, U.S.A.) located in a field-based laboratory container at the Ketzin site. The gas flow was split at the outlet of the GC system by a union tee to an OmniStar quadrupole MS gas analyzer (Pfeiffer Vacuum GmbH, Asslar, Germany) and the Delta Ray mid-IR laser instrument (Thermo Scientific, Bremen, Germany).

At daily intervals the riser tube was disconnected from the GC system to fill a 12 mL Labco Exetainer with gas-tight butyl rubber septa (Labco Ltd., Lampeter, U.K.). The vials were flushed with CO₂ from the storage formation in flow-through mode for 5 min by two needles that pierced the septa. When this sampling was completed the riser tube was reconnected before the next IRIS

measurement. In total 11 samples were collected and then analyzed for their $^{13}\text{C}/^{12}\text{C}$ ratio by IRMS in November 2013 at the University Erlangen-Nürnberg. Published data on storage effects of Exetainers vials with butyl rubber septa show that the used vial–septum combination is gastight and isotope composition is stable from several weeks^{26,27} up to a period of 6 months.²⁸ The data were then compared to the data acquired in the field with the mid-IR laser instrument.

Isotope Ratio Mass Spectrometry. All stable isotope values are reported in the standard δ -notation as deviations in per mil (‰) from the reference material Vienna Pee Dee Belemnite (VPDB) according to

$$\delta = \frac{R_{\text{sample}}}{R_{\text{reference}}} - 1 \quad (1)$$

where R is the ratio of the numbers (n) of the heavy and light isotope of an element [e.g., $n(^{13}\text{C})/n(^{12}\text{C})$] in the sample and the reference.²⁹

In the laboratory, gas was extracted from the Exetainers that were filled at the Ketzin pilot site with a gastight syringe and transferred into Exetainers that were prefilled with helium. Samples were analyzed on a Thermo Delta V Advantage IRMS coupled to a Gasbench II in continuous flow mode (Thermo Scientific, Bremen, Germany). Isotope values were normalized to the VPDB scale by a two-point calibration³⁰ based on two in-house calcite reference materials that were calibrated directly against NBS-19 and LSVEC.^{31,32} For calibration a $\delta^{13}\text{C}$ value of +1.95‰ and −46.6‰ was assigned to NBS-19 and LSVEC, respectively.

All samples were analyzed in duplicate, and the reported value is the mean value. Offset between duplicates was lower than 0.05‰. Control samples were prepared in an analogous manner to the Ketzin samples from high-purity (99.995%) CO_2 and helium-flushed 12 mL Exetainer vials. These samples were placed at regular intervals in the analytical sequence. Reproducibility based on the repeat measurement of these control samples was 0.03‰ ($\pm 1\sigma$, $n = 6$). The long-term analytical precision of the IRMS system is ± 0.15 ‰.

The $\delta^{13}\text{C}$ value of CO_2 used for the control sample was calibrated independently by dual inlet mass spectrometry against international isotope reference CO_2 RM8562 from the International Atomic Energy Agency (IAEA). Accuracy of the control sample was within 1σ analytical precision, i.e., the difference of the control sample average and the defined $\delta^{13}\text{C}$ value for this gas was smaller than 0.15‰.

Mid-Infrared Isotope Ratio Spectroscopy. The laser light of the Delta Ray instrument is generated by a difference frequency generation (DFG) mid-infrared laser that operates at $4.3\ \mu\text{m}$ with a power of $\sim 2\ \mu\text{W}$. The absorption lines of the different carbon dioxide isotopologues are shifted relative to each other and allow for the calculation of their relative abundance and the stable isotope ratios from the spectrum (Figure 2). The tunable mid-infrared laser beam is generated by two near-infrared telecommunication type lasers that are mixed in periodically poled lithium niobate (PPLN). One laser is frequency-stabilized, while the other is a tunable distributed feedback (DFB) laser that is used to tune the mid-infrared difference frequency. The laser scans over the absorption lines at 500 Hz and the signal is averaged for 1 s before the spectrum is fitted and isotope ratios are calculated from the spectrum fit. The sample gas is measured for its concentration and isotope composition by laser direct absorption in a multipass Herriot cell with an effective path

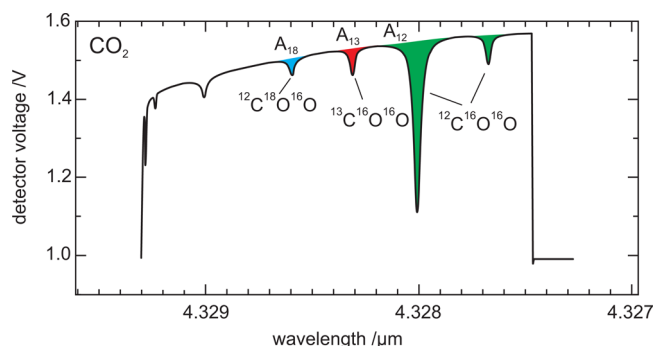


Figure 2. Mid-infrared spectral region at a wavelength of $4.3\ \mu\text{m}$. The laser scans over the absorption lines at 500 Hz. The stable isotope ratios of carbon dioxide can be calculated from the respective peak areas of the different isotopologues.

length of about 5 m (Figure 3). The detector is located outside of the gas cell. The cell temperature is controlled at $37\ ^\circ\text{C}$ within a

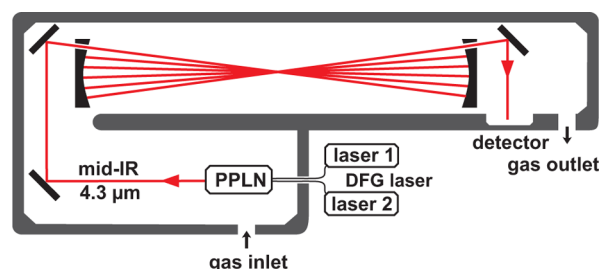


Figure 3. Principle optical layout scheme of the Delta Ray instrument (Thermo Scientific, Bremen, Germany) based on tunable laser direct absorption in the mid-infrared. The figure was simplified for clarity. The difference frequency generation (DFG) laser source operates at $4.3\ \mu\text{m}$. Two near-infrared wavelengths are mixed in periodically poled lithium niobate (PPLN) to generate mid-infrared laser light. The Herriot cell length is $\sim 40\ \text{cm}$, and effective optical path length is $\sim 5\ \text{m}$ (14 pass). See text for further details.

range of a few millikelvin, and the pressure is controlled at 100 mbar. The sample line runs through the temperature-controlled enclosure that allows for thermal equilibration before the sample gas enters the cell. The principle of the mid-infrared DFG laser platform that is used inside the instrument is described in detail by Scherer et al.³³ The required sample gas flow is $80\ \text{mL min}^{-1}$ with a cell exchange time of 35 s. The operating concentration range is 200–3500 ppmV with an available optional dilution module for higher concentrations.

In direct absorption laser spectroscopy, the calculated isotope ratios are dependent on the CO_2 concentration.^{34,35} That means that the measured δ -value of a gas with a uniform ^{13}C to ^{12}C ratio will change as CO_2 concentration changes. This effect is typically referred to as linearity. To receive accurate and high-precision data it is crucial to account for this effect. The Delta Ray instrument addresses this issue in two ways: (1) The reference gas CO_2 concentration is automatically adjusted to match the sample gas concentration by the instruments software, and (2) the instrument is equipped with a universal reference interface (URI) that automatically determines the nonlinearity of the system by diluting the reference gases with CO_2 -free synthetic air. During a reference cycle (see below), the concentration of the reference gases is set to the average concentration during the last minute before the reference measurement. While procedure 1 removes the nonlinearity of the system to first order, secondary

effects are corrected by the linearity correction function determined by procedure 2.

Typical instruments precision, i.e., how close the individual measurements agree,³⁶ is demonstrated by an Allan–Werle plot (Figure 4). This concept is used to characterize accuracy and

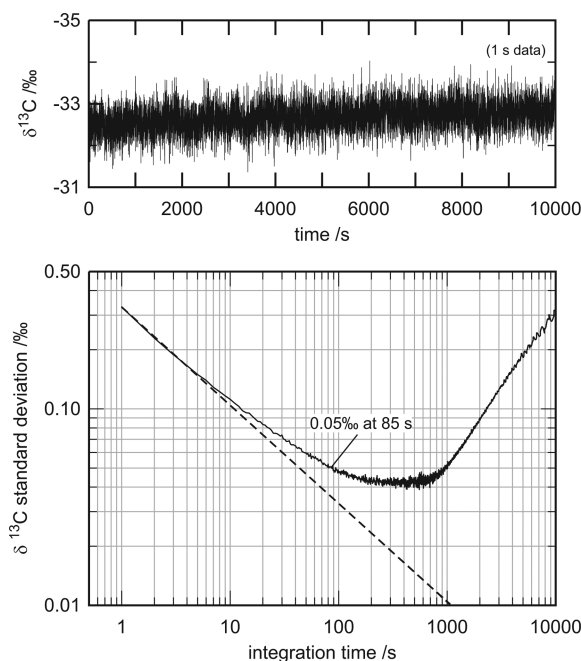


Figure 4. $\delta^{13}\text{C}$ time series and Allan–Werle plot (ref 37) for a typical mid-IR laser spectrometer used in this study. At 12 s integration time the precision for $\delta^{13}\text{C}$ is 0.1‰ and better than 0.05‰ after 85 s. Maximum precision of 0.039‰ is reached at 554 s. The dashed line shows the theoretical shot-noise limit.

precision of laser spectrometers and is described in detail by Werle.³⁷ Precision for 15 s integration time is typically better than 0.1‰ for $\delta^{13}\text{C}$, but exact time may vary slightly for the individual instrument. The sample is referenced to the VPDB scale directly in the instrument by a two-point calibration derived from two calibrated CO_2 reference gases with high and low isotope values that are connected to the analyzer. The reference gas cylinders are filled with gaseous CO_2 so that fractionation effects due to temperature changes are excluded. This potential source of error by using CO_2 cylinders that contain liquid CO_2 is avoided here. The volume of reference cylinders is enough to allow for weeks to months of unattended operation, depending on the recalibration frequency.

Between August 16 and 27, 2013, the instrument was connected to the CO_2 riser tube by a union tee behind the GC gas analyzer at the Ketzin pilot site. The CO_2 sample gas flow from the reservoir was diluted by zero air (20.5% oxygen in nitrogen) to meet the specified CO_2 concentration range of the instrument and was set to (2200 ± 150) ppmV. Reservoir CO_2 was measured with an averaging time of 25 min followed by a 5 min reference measurement. For averaging 5 min of isotope ratio measurements were integrated, and 5 of these averages were averaged into a single data point. The result is a $\delta^{13}\text{C}$ curve with 30 min resolution over the 10 day measurement campaign (Figure 5).

Differences between corresponding IRIS and IRMS data pairs are expressed as

$$\Delta\delta = \delta_{\text{IRIS}} - \delta_{\text{IRMS}} \quad (2)$$

RESULTS AND DISCUSSION

Laser Spectroscopy. The $\delta^{13}\text{C}$ -IRIS data series with 30 min resolution is shown in Figure 5. During this 10 day monitoring campaign the $\delta^{13}\text{C}$ values ranged between -28‰ and -10‰ . Initial values on August 16 were about -25.5‰ and showed a continuous rise to -21.5‰ on the morning of August 20. The laser instrument did not operate between August 16 5:00 p.m. and August 18 10:30 a.m. due to a software problem that caused a shutdown and required a remote restart of the system.

On the morning of August 20 the recorded $\delta^{13}\text{C}$ values started to rise quickly and reached a maximum of -9.8‰ in the late afternoon followed by a decline to values between -18‰ and -20‰ . This pronounced positive shift was the result of a change in borehole conditions on this day. It was noticed during the experiment that water in the borehole prevented a direct CO_2 delivery from the reservoir to the surface. The water was removed on August 20, and afterward the full formation gas pressure applied at the riser tube. Therefore, $\delta^{13}\text{C}$ values of CO_2 that were measured until August 20 might not have reflected changes in the reservoir but were masked by fractionation processes between gaseous CO_2 and dissolved inorganic carbon species^{38,39} that occur during dissolution of CO_2 in the fluid that filled the riser tube. After removal of the water, the riser tube was directly connected to the reservoir and $\delta^{13}\text{C}$ values were more variable with several relatively short and sharp positive excursions of several per mil that lasted for about 3 to 4 h.

The observed positive excursions are likely caused by arrival of portions from the injected tracer CO_2 with high $\delta^{13}\text{C}$ values. The overall trend of declining $\delta^{13}\text{C}$ values after August 20 indicates that the major peak of the tracer might have already passed the observation well. The short-term excursions that accompanied the decline of $\delta^{13}\text{C}$ toward the reservoir baseline values of $\sim -28.5\text{‰}$ are comparable to flow patterns of gas tracers (sulfur hexafluoride and krypton) that were coinjected with CO_2 into a deep saline aquifer at the EOR Cranfield test site.⁴⁰ At Cranfield, reservoir heterogeneity caused a complex arrival pattern of the injected tracer gases with a series of temporary increases superimposed on overall downward trends. Lu et al.⁴⁰ showed that the compositional fluctuations were caused by migration along separate and distinct preferential flow paths between injection well and observation site. The $\delta^{13}\text{C}$ isotope tracer signal of this study appears to reflect a comparable CO_2 migration behavior in the heterogeneous reservoir at the Ketzin site.

Some of the positive excursions seem to roughly correspond with IRMS sampling time suggesting that they might also be sampling artifacts caused by air entering the IRIS system during Exetainer filling. Although possible, this option is not very likely because positive excursions were also measured in time intervals without IRMS sampling and not all Exetainer samplings were followed by a positive excursion. This supports our interpretation that the observed dynamic pattern is related to the complex arrival pattern of the injected CO_2 .

Comparison with IRMS. For comparison of $\delta^{13}\text{C}$ values measured by the new mid-infrared laser spectrometer and conventional IRMS technique the results from the $\delta^{13}\text{C}$ -IRMS values are plotted together with the nearest $\delta^{13}\text{C}$ -IRIS value measured prior to Exetainer filling (Figure 5). Note that in reality filling of Exetainers occurred a few minutes later than the corresponding IRIS measurement. For better visibility the relevant time intervals are enlarged in Figure 6. Corresponding

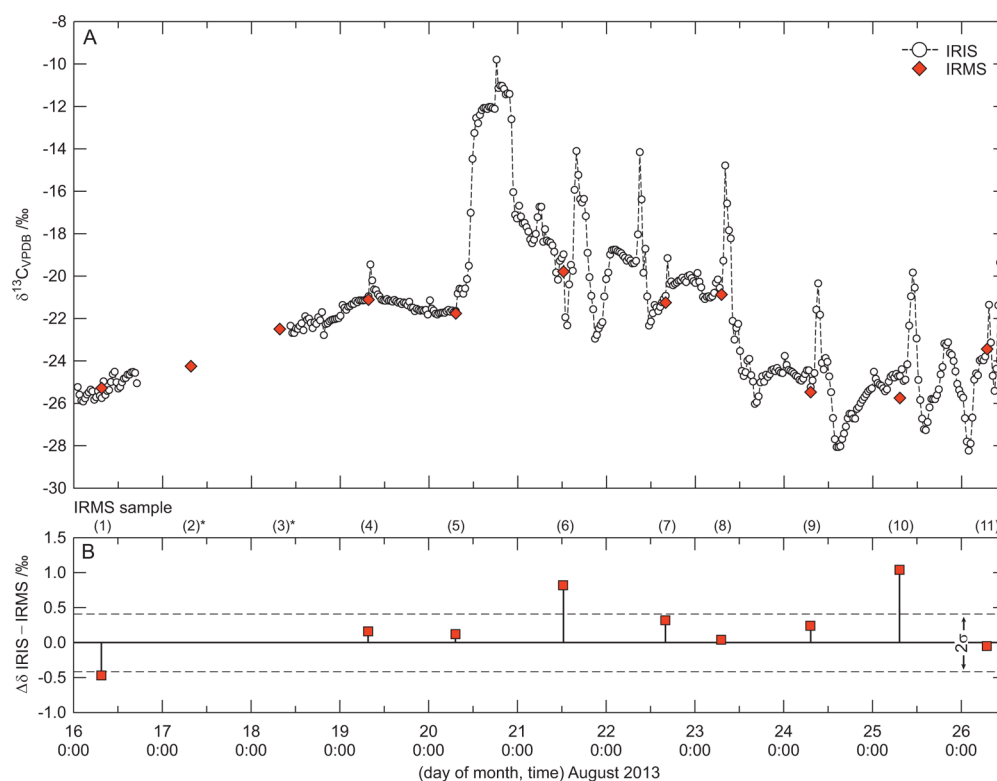


Figure 5. (A) $\delta^{13}\text{C}_{\text{CO}_2}$ values measured in situ at Ktzi 203 by isotope ratio infrared spectroscopy (IRIS; Delta Ray) and from Labco Exetainers by conventional isotope ratio mass spectrometry (IRMS; Gasbench II–Delta V Advantage). Symbol size includes $\pm 1\sigma$ analytical precision. (B) Difference between corresponding IRIS and IRMS data. Samples 2 and 3 are marked with an asterisk because they do not have a corresponding IRIS value.

δ -values between IRIS and IRMS ($\Delta\delta$) are listed in Table 1, and differences are shown in Figure 5B.

The 2σ precision for IRMS analyses in this study is 0.3‰ (see the Experimental Section), and an identical value is reported for the IRIS instrument by the manufacturer for 30 replicates with 60 s integration time. Therefore, the combined 2σ analytical uncertainty of both systems is calculated with 0.42‰ here.⁴¹ Six out of nine IRIS–IRMS pairs overlap within 2σ analytical uncertainty. Therefore, these values are not distinguishable by analytical means. Note that for IRMS samples 2 and 3 no corresponding IRIS data exist. Nevertheless, these samples seem to perfectly bridge the IRIS data gap.

The IRIS data indicate that $\delta^{13}\text{C}$ values of injected CO_2 that is lifted to the earth surface again at the observation well Ktzi 203 fluctuated over several per mil within short time intervals. Here, the continuous laser isotope record revealed hitherto unknown $\delta^{13}\text{C}$ dynamics. Sampling time of IRIS and IRMS data points in Figure 5 does not coincide exactly due to the sampling procedure. To account for that time lag, the IRMS values were compared to the IRIS values measured before the filling of the Exetainers (see above). However, in the case of a rather rapid $\delta^{13}\text{C}$ shift, the gas sampled to Exetainers could already hold a slightly different $\delta^{13}\text{C}$ value than the gas measured by the laser instrument a few minutes before. In that case, the isotopic composition of the IRMS sample should plot between the corresponding and the subsequent IRIS sample that shows the more positive or negative $\delta^{13}\text{C}$ values. Such a pattern is observed for sample pairs 1 and 6 (Figure 6), and this might explain the relatively large offsets of 0.5‰ and 0.8‰ observed for these IRIS–IRMS pairs. For example, IRIS data showed a sharp negative 3‰ excursion directly during the time interval in which

IRMS sample 6 was filled (Figure 6), and this shift might have already started during the filling of the IRMS sample.

IRMS sample 10 shows the maximum $\Delta\delta$ value of 1.0‰ from the IRIS data. This value is larger than for every other sample pairing. Here it is obvious from the IRIS data that no sudden $\delta^{13}\text{C}$ shifts occurred during this sample interval on August 8 that could explain the observed offset as discussed above for IRMS samples 1 and 6.

Nonparametric statistical tests for normality (e.g., Shapiro–Wilk⁴² or Anderson–Darling⁴³) indicate that $\Delta\delta$ values are normally distributed. A boxplot of the residuals of all IRIS–IRMS pairs (Figure 7) shows that the $\Delta\delta$ value for IRMS sample 10 does not meet the suspected outlier criteria of $1.5 \times$ interquartile range (IQR) above the third quartile (i.e., $>1.43\text{‰}$).⁴⁴ In other words, descriptive statistics do not designate this sample as an outlier. Repeat analyses of the gas sample confirmed the $\delta^{13}\text{C}$ –IRMS value. In addition, chromatograms did not indicate corruption of the sample by infiltration of air through a leaking septa. The most likely interpretation from the available data is that the error was already introduced during filling of the sample vial although the exact reason remains unclear.

CONCLUSIONS

In this study real samples taken during a CCS monitoring campaign were used to evaluate the performance of the laser instrument under realistic working conditions at a field-based container and in continuous 24 h/7day operation mode. Overall, the $\delta^{13}\text{C}$ results between conventional IRMS technique and the new mid-infrared laser spectrometer agree remarkably well within the errors of measurement. This proves the capability of the new mid-infrared direct absorption technique to measure

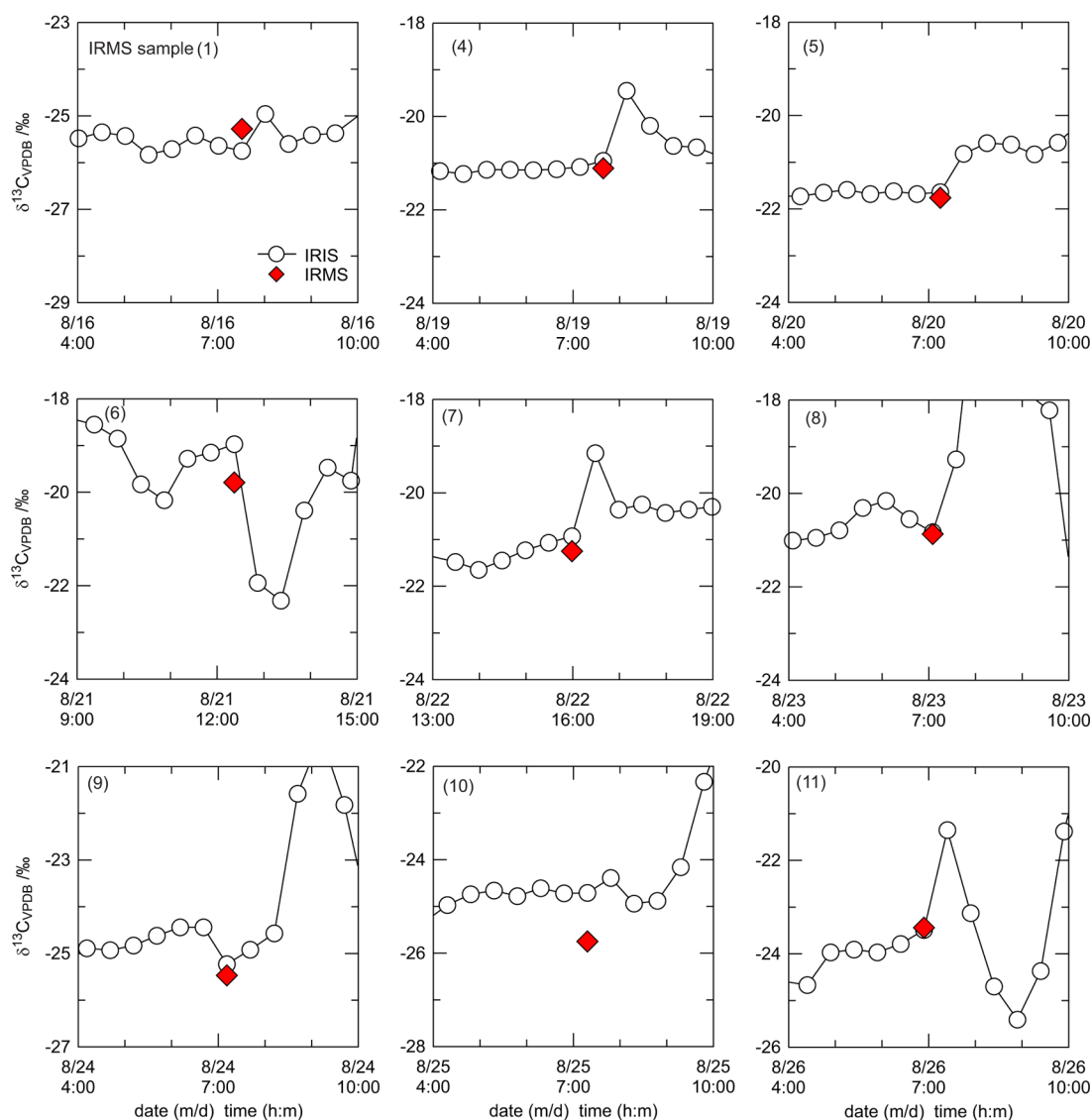


Figure 6. Time interval with enlarged $\delta^{13}\text{C}$ -IRMS analyses. Symbol size includes $\pm 1\sigma$ analytical precision.

Table 1. Comparison of $\delta^{13}\text{C}$ Values Measured at the Ketzin Pilot Site by Isotope Ratio Infrared Spectroscopy (IRIS) and Laboratory Analyses by Isotope Ratio Mass Spectrometry (IRMS)^a

sample ID	date time	IRIS $\delta^{13}\text{C}_{\text{VPDB}} \text{ ‰}$	IRMS $\delta^{13}\text{C}_{\text{VPDB}} \text{ ‰}$	offset $\Delta\delta \text{ ‰}$
1	Aug 16, 2013 07:31	-25.75	-25.28	-0.47
2	Aug 17, 2013 07:40	<i>b</i>	-24.25	<i>b</i>
3	Aug 18, 2013 07:40	<i>b</i>	-22.50	<i>b</i>
4	Aug 19, 2013 07:39	-20.95	-21.11	0.16
5	Aug 20, 2013 07:15	-21.64	-21.76	0.12
6	Aug 21, 2013 12:22	-18.97	-19.79	0.82
7	Aug 22, 2013 15:59	-20.93	-21.25	0.32
8	Aug 23, 2013 07:05	-20.83	-20.87	0.04
9	Aug 24, 2013 07:41	-25.23	-25.47	0.24
10	Aug 25, 2013 07:48	-24.71	-25.75	1.04
11	Aug 26, 2013 06:54	-23.49	-23.44	-0.05

^aVPDB: Vienna Pee Dee Belemnite. ^bIRIS instrument was not working in this time interval.

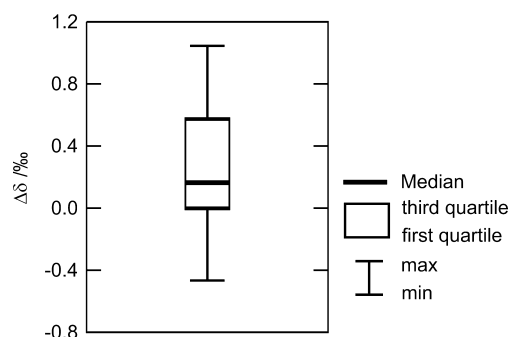


Figure 7. Median-based box-and-whisker diagram of isotope data differences ($\Delta\delta$). Suspected outlier criterion after Tukey (ref 44). Shapiro–Wilk’s test for normality (ref 42) indicates that data is normally distributed ($W = 0.94$; $p = 0.57$; $n = 9$). Median is 0.16‰ . IQR—interquartile range.

high precision and accurate real-time stable isotope data directly in the field.

Sufficient time resolution during any kind of monitoring is fundamental for the detection of changes in the parameters of

interest. The required time resolution is defined by the time interval at which changes potentially will occur. Previous studies showed that changes of gas tracers can occur within days or even hours.^{40,45} Existing stable isotope studies from the Ketzin pilot site that used conventional IRMS analyses^{5–7} showed that $\delta^{13}\text{C}$ values of injected CO_2 could be used as a natural occurring tracer signal because injected CO_2 originated from two different sources with largely different $\delta^{13}\text{C}$ values. However, the applied method was limited by sample acquisition, because sampling for IRMS analyses into individual Exetainers must be done manually on site and is noncontinuous. In addition, stable isotope sampling only occurred during defined monitoring campaigns. It is therefore likely that dispersed tracer signals in periods between monitoring campaigns or short-term variances as observed in this study were missed during previous works.

The observation well Ktzi 203 that was sampled in this study is the latest of the several wells drilled at Ketzin and is located only at a distance of 20 m to the injection well. The IRIS and IRMS data of this study are the first stable isotope analyses from this observation well. Multiple shifts of several per mil were recorded by on-site IRIS measurement with 30 min resolution and were confirmed by daily IRMS analyses.

This monitoring data set would not have been as complete if IRMS analyses only have been used. Laser spectroscopy data revealed a much more intensive dynamic with fast changing $\delta^{13}\text{C}$ values. This dynamic flow pattern is in accordance with observations revealed by continuous conventional gas tracer monitoring at other CO_2 injection sites and reflects the arrival of the tracer through preferential flow paths. However, possible causes of the newly found dynamic tracer signal must be investigated in future studies and could contribute to a better tracing of the migration of the underground CO_2 plume. This would help to ensure the long-term integrity of the reservoir. The required detailed data logging will probably be only possible with robust field deployable stable isotope analyzers that deliver reliable, accurate, and real-time in situ data. The tested new mid-infrared laser spectrometer fulfilled these requirements.

Finally, the new mobile, laser-based isotope instrument opens several possibilities in various other scientific fields beyond CCS monitoring. Recently, the instrument was successfully used to perform real-time data of volcanic CO_2 at Mt. Etna,⁴⁶ but numerous other applications such as carbon cycle studies, urban monitoring, ecology studies, or atmospheric greenhouse gas research are imaginable.

AUTHOR INFORMATION

Corresponding Author

*E-mail: robert.van.geldern@fau.de. Phone +49 9131 8522514. Fax +49 9131 29294.

Notes

The authors declare the following competing financial interest(s): H.J.J. discloses that he is employed by Thermo Fisher Scientific, the manufacturer of the Delta Ray laser isotope analyzer.

ACKNOWLEDGMENTS

We thank C. Hanke, L. Wunder, J. de Wendt (FAU), and B. Plessen (GFZ) for their help with sampling and laboratory analyses. The authors thank the interdisciplinary research team working on the Ketzin project. Parts of this study were funded by the German Ministry of Education and Research (BMBF) project CO_2 ISO-LABEL (Grant No. 03G0801A) and CO_2 MAN

(Grant No. 03G0760B), and the grant for major instrumentation to the chair of Applied Geology (INST 90/678-1 FUGG). We also thank the three reviewers for their helpful comments.

REFERENCES

- (1) Le Quéré, C.; Peters, G. P.; Andres, R. J.; Andrew, R. M.; Boden, T. A.; Ciais, P.; Friedlingstein, P.; Houghton, R. A.; Marland, G.; Moriarty, R.; Sitch, S.; Tans, P.; Arneeth, A.; Arvanitis, A.; Bakker, D. C. E.; Bopp, L.; Canadell, J. G.; Chini, L. P.; Doney, S. C.; Harper, A.; Harris, I.; House, J. I.; Jain, A. K.; Jones, S. D.; Kato, E.; Keeling, R. F.; Klein Goldewijk, K.; Körtzinger, A.; Koven, C.; Lefèvre, N.; Maignan, F.; Omar, A.; Ono, T.; Park, G. H.; Pfeil, B.; Poulter, B.; Raupach, M. R.; Regnier, P.; Rödenbeck, C.; Saito, S.; Schwinger, J.; Segschneider, J.; Stocker, B. D.; Takahashi, T.; Tilbrook, B.; van Heuven, S.; Viovy, N.; Wanninkhof, R.; Wiltshire, A.; Zaehle, S. *Earth Syst. Sci. Data* **2014**, *6* (1), 235–263 DOI: 10.5194/essd-6-235-2014.
- (2) IPCC. *Climate Change 2013—The Physical Science Basis*. Working Group I Contribution to the Fifth Assessment Report of the Intergovernmental Panel on Climate Change (IPCC); Cambridge University Press: New York, 2013, pp 1535.
- (3) NOAA Carbon Dioxide at NOAA's Mauna Loa Observatory reaches new milestone: Tops 400 ppm. <http://research.noaa.gov/News/NewsArchive/LatestNews/TabId/684/ArtMID/1768/ArticleID/10061/Carbon-Dioxide-at-NOAAs-Mauna-Loa-Observatory-reaches-new-milestone-Tops-400-ppm.aspx> (accessed August 15, 2014).
- (4) Haszeldine, R. S. *Science* **2009**, *325* (5948), 1647–1652 DOI: 10.1126/science.1172246.
- (5) Nowak, M.; van Geldern, R.; Myrtilinen, A.; Zimmer, M.; Barth, J. A. C. *Appl. Geochem.* **2014**, *47*, 44–51 DOI: 10.1016/j.apgeochem.2014.05.009.
- (6) Myrtilinen, A.; Becker, V.; van Geldern, R.; Würdemann, H.; Morozova, D.; Zimmer, M.; Taubald, H.; Blum, P.; Barth, J. A. C. *Int. J. Greenhouse Gas Control* **2010**, *4* (6), 1000–1006 DOI: 10.1016/j.ijggc.2010.02.005.
- (7) Nowak, M.; Myrtilinen, A.; Zimmer, M.; Wiese, B.; van Geldern, R.; Barth, J. A. C. *Energy Procedia* **2013**, *40*, 346–354 DOI: 10.1016/j.egypro.2013.08.040.
- (8) Emberley, S.; Hutcheon, I.; Shevalier, M.; Durocher, K.; Mayer, B.; Gunter, W. D.; Perkins, E. H. *Appl. Geochem.* **2005**, *20* (6), 1131–1157 DOI: 10.1016/j.apgeochem.2005.02.007.
- (9) Raistrick, M.; Mayer, B.; Shevalier, M.; Perez, R. J.; Hutcheon, I.; Perkins, E.; Gunter, B. *Environ. Sci. Technol.* **2006**, *40* (21), 6744–6749 DOI: 10.1021/es060551a.
- (10) Chesson, L. A.; Bowen, G. J.; Ehleringer, J. R. *Rapid Commun. Mass Spectrom.* **2010**, *24* (21), 3205–3213 DOI: 10.1002/rcm.4759.
- (11) Wen, X. F.; Meng, Y.; Zhang, X. Y.; Sun, X. M.; Lee, X. *Atmos. Meas. Tech.* **2013**, *6* (6), 1491–1501 DOI: 10.5194/amt-6-1491-2013.
- (12) van Geldern, R.; Barth, J. A. C. *Limnol. Oceanogr.: Methods* **2012**, *10*, 1024–1036 DOI: 10.4319/lom.2012.10.1024.
- (13) Wassenaar, L. I.; Ahmad, M.; Aggarwal, P.; van Duren, M.; Pölsenstein, L.; Araguas, L.; Kurtas, T. *Rapid Commun. Mass Spectrom.* **2012**, *26* (15), 1641–1648 DOI: 10.1002/rcm.6270.
- (14) Wassenaar, L. I.; Coplen, T. B.; Aggarwal, P. K. *Environ. Sci. Technol.* **2014**, *48* (2), 1123–1131 DOI: 10.1021/es403354n.
- (15) Gröning, M. *Rapid Commun. Mass Spectrom.* **2011**, *25*, 2711–2720 DOI: 10.1002/rcm.5074.
- (16) Krevor, S.; Perrin, J.-C.; Esposito, A.; Rella, C.; Benson, S. *Int. J. Greenhouse Gas Control* **2010**, *4* (5), 811–815 DOI: 10.1016/j.ijggc.2010.05.002.
- (17) McAlexander, I.; Rau, G. H.; Liem, J.; Owano, T.; Fellers, R.; Baer, D.; Gupta, M. *Anal. Chem.* **2011**, *83* (16), 6223–6229 DOI: 10.1021/ac2007834.
- (18) Jackson, R. B.; Down, A.; Phillips, N. G.; Ackley, R. C.; Cook, C. W.; Plata, D. L.; Zhao, K. *Environ. Sci. Technol.* **2014**, *48* (3), 2051–2058 DOI: 10.1021/es404474x.

- (19) Phillips, N. G.; Ackley, R.; Crosson, E. R.; Down, A.; Hutyra, L. R.; Brondfield, M.; Karr, J. D.; Zhao, K.; Jackson, R. B. *Environ. Pollut.* **2013**, *173* (0), 1–4 DOI: 10.1016/j.envpol.2012.11.003.
- (20) Vogel, F. R.; Huang, L.; Ernst, D.; Giroux, L.; Racki, S.; Worthy, D. E. J. *Atmos. Meas. Technol.* **2013**, *6* (2), 301–308 DOI: 10.5194/amt-6-301-2013.
- (21) Griffis, T. J. *Agric. For. Meteorol.* **2013**, *174–175* (0), 85–109 DOI: 10.1016/j.agrformet.2013.02.009.
- (22) Jost, H.-J.; Wapelhorst, E.; Schlueter, H.-J.; Kracht, O.; Radke, J.; Hilker, A.; Barth, J. A. C.; van Geldern, R.; Nowak, M. E.; Zimmer, M.; Szizybalski, A. Performance of an isotope ratio infrared spectrometer for simultaneous measurements of carbon and oxygen isotopologues of CO₂. Abstracts of the EGU General Assembly 2014, Vienna, Austria; Geophysical Research Abstracts: Vienna, Austria, 2014; pp EGU2014–16071–1.
- (23) Martens, S.; Kempka, T.; Liebscher, A.; Lüth, S.; Möller, F.; Myrntinen, A.; Norden, B.; Schmidt-Hattenberger, C.; Zimmer, M.; Kühn, M. *Environ. Earth Sci.* **2012**, *67* (2), 323–334 DOI: 10.1007/s12665-012-1672-5.
- (24) Martens, S.; Liebscher, A.; Möller, F.; Henningses, J.; Kempka, T.; Lüth, S.; Norden, B.; Prevedel, B.; Szizybalski, A.; Zimmer, M.; Kühn, M.; Ketzin Group. *Energy Procedia* **2013**, *37*, 6434–6443. <http://doi.org/10.1016/j.egypro.2013.06.573>.
- (25) Wiese, B.; Zimmer, M.; Nowak, M.; Pellizzari, L.; Pilz, P. *Environ. Earth Sci.* **2013**, *70* (8), 3709–3726 DOI: 10.1007/s12665-013-2744-x.
- (26) Spötl, C. *Rapid Commun. Mass Spectrom.* **2004**, *18* (11), 1239–1242 DOI: 10.1002/rcm.1468.
- (27) Spötl, C. *Isot. Environ. Health Stud.* **2005**, *41* (3), 217–221 DOI: 10.1080/10256010500230023.
- (28) Taipale, S. J.; Sonninen, E. *Rapid Commun. Mass Spectrom.* **2009**, *23* (16), 2507–2510 DOI: 10.1002/rcm.4072.
- (29) Coplen, T. B. *Rapid Commun. Mass Spectrom.* **2011**, *25* (17), 2538–2560 DOI: 10.1002/rcm.5129.
- (30) Paul, D.; Skrzypek, G.; Fórizs, I. *Rapid Commun. Mass Spectrom.* **2007**, *21* (18), 3006–3014.
- (31) Coplen, T. B.; Brand, W. A.; Gehre, M.; Gröning, M.; Meijer, H. A. J.; Toman, B.; Verkouteren, R. M. *Anal. Chem.* **2006**, *78* (7), 2439–2441 DOI: 10.1021/ac052027c.
- (32) IAEA, Reference Material Online Catalog. <http://nucleus.iaea.org/rpst/ReferenceProducts/ReferenceMaterials/index.htm> (accessed August 18, 2014).
- (33) Scherer, J. J.; Paul, J. B.; Jost, H. J.; Fischer, M. L. *Appl. Phys. B: Lasers Opt.* **2013**, *110* (2), 271–277 DOI: 10.1007/s00340-012-5244-x.
- (34) Tuzson, B.; Mohn, J.; Zeeman, M. J.; Werner, R. A.; Eugster, W.; Zahniser, M. S.; Nelson, D. D.; McManus, J. B.; Emmenegger, L. *Appl. Phys. B: Lasers Opt.* **2008**, *92* (3), 451–458 DOI: 10.1007/s00340-008-3085-4.
- (35) Nelson, D. D.; McManus, J. B.; Herndon, S. C.; Zahniser, M. S.; Tuzson, B.; Emmenegger, L. *Appl. Phys. B: Lasers Opt.* **2008**, *90* (2), 301–309 DOI: 10.1007/s00340-007-2894-1.
- (36) VIM International vocabulary of metrology—Basic and general concepts and associated terms (VIM), 3rd ed. (JCGM 200:2012). <http://www.bipm.org/en/publications/guides/vim.html> (accessed August 18, 2014).
- (37) Werle, P. *Appl. Phys. B: Lasers Opt.* **2011**, *102* (2), 313–329 DOI: 10.1007/s00340-010-4165-9.
- (38) Myrntinen, A.; Becker, V.; Barth, J. A. C. *Earth-Sci. Rev.* **2012**, *115* (3), 192–199 DOI: 10.1016/j.earscirev.2012.08.004.
- (39) Becker, V.; Myrntinen, A.; Blum, P.; van Geldern, R.; Barth, J. A. C. *Int. J. Greenhouse Gas Control* **2011**, *5* (5), 1250–1258 DOI: 10.1016/j.ijggc.2011.05.001.
- (40) Lu, J.; Cook, P. J.; Hosseini, S. A.; Yang, C.; Romanak, K. D.; Zhang, T.; Freifeld, B. M.; Smyth, R. C.; Zeng, H.; Hovorka, S. D. J. *Geophys. Res.: Solid Earth* **2012**, *117* (B3), B03208 DOI: 10.1029/2011JB008939.
- (41) Ku, H. H. J. *Res. Natl. Bur. Stand. (U. S.)* **1966**, *70C* (4), 263–273 DOI: 10.6028/jres.070c.025.
- (42) Shapiro, S. S.; Wilk, M. B. *Biometrika* **1965**, *52*, 591–611 DOI: 10.1093/biomet/52.3-4.591.
- (43) Anderson, T. W.; Darling, D. A. *Ann. Math. Stat.* **1952**, 193–212 DOI: 10.1214/aoms/1177729437.
- (44) Tukey, J. W. *Exploratory Data Analysis*; Addison-Wesley: Reading, MA, 1977.
- (45) Zimmer, M.; Erzinger, J.; Kujawa, C. *Int. J. Greenhouse Gas Control* **2011**, *5* (4), 995–1001 DOI: 10.1016/j.ijggc.2010.11.007.
- (46) Rizzo, A. L.; Jost, H.-J.; Caracausi, A.; Paonita, A.; Liotta, M.; Martelli, M. *Geophys. Res. Lett.* **2014**, *41* (7), 2014GL059722 DOI: 10.1002/2014GL059722.